Microscopy of electronic states contributing to lasing in ridge quantum-wire laser structure

Shinichi Watanabe,[a] Shyun Koshiba,[b] Masahiro Yoshita, Hiroyuki Sakaki,[c] Motoyoshi Baba, and Hidefumi Akiyama
Institute for Solid State Physics, University of Tokyo, 5-1-5, Kashiwanoha, Kashiwa, Chiba 277-8581, Japan

(Received 17 May 1999; accepted for publication 10 August 1999)

Distribution of electronic states inside ridge quantum-wire (QWR) laser cavity was investigated using spatially and spectrally resolved top-view photoluminescence (PL) imaging method. PL inhomogeneity in QWR has shown that the electronic states were perturbed by the fluctuation of vertical thickness in the scale of ~nm, while the optical waveguide was not. The PL images of QWR were traced up to the lasing condition to examine the lasing origin. © *1999 American Institute of Physics.* [S0003-6951(99)00541-0]

Nanoscale laser devices based on one-dimensional (1D) quantum wire (QWR) structures have been fabricated[1–7] aimed at realizing novel laser performances. Microspectroscopy investigation on the spatial origin of both emission and lasing is important in such QWR laser structures, since adjacent quantum well (QW) structures exist beside QWR structures and there is a need to determine which part contributes to the stimulated emission. We have previously demonstrated photoluminescence (PL) imaging measurement of ridge QWR laser structures from the cleaved edges, and successfully separated PL of QWRs with that of adjacent QWs with spatial resolution of 1 μm.[8] The pattern of stimulated emission from the cleaved edge was also studied to assign the origin of the lasing. Recently, near-field scanning optical microscopy has been used to investigate PL and lasing modes from the cleaved edges of T-shaped and V-groove QWR laser structures.[9,10]

Also important in microspectroscopy investigations of those laser structures is the spatial distribution, or the uniformity, of electronic states along the wire direction, since lasing is a cooperative phenomenon of the entire electronic state in the laser cavity. In this article, we present spectrally and spatially resolved top-view PL imaging measurements of ridge QWR laser structures under lasing and prelasing conditions, and confirm that the origin of lasing is the transition between excited states of the QWR.

Figure 1(a) shows a cross-sectional transmission electron microscope (TEM) image of a ridge QWR laser structure. Separately confined-heterostructure (SCH) layers were formed. The core layer of the SCH was composed of a GaAs active layer with a nominal vertical thickness of 5 nm sandwiched by 90 nm thick barrier layers of an $Al_{0.2}Ga_{0.8}As$ digital alloy. As a result, the QWR is formed at the ridge corner of the two adjacent QWs (side-QWs). The core layer was sandwiched by the cladding layers of the $Al_{0.4}Ga_{0.6}As$ digital alloy to construct SCH optical waveguides.[7] The sample was cleaved to form optical cavities of length $L=300\,\mu$m. As shown in Fig. 1(a), we define the *x* axis as the wire direction, the *y* axis as the lateral confinement direction, and the *z* axis as the growth direction.

Figure 1(b) shows the emission and lasing spectra of ridge QWR laser structures at $T=8.9$ K, under optical excitation by Ti:Al_2O_3 laser pulses with a photon energy of 1.769 eV [indicated by an arrow in Fig. 1(b)], a repetition rate of 76 MHz, and a pulse duration of 200 fs. The experimental configuration of optical excitation was the same as Ref. 8 except for the laser pump source. Direct excitation of carriers in the side-QWs made it possible to estimate the carrier density inside the active regions. Taking into account a reflectance of 30% at the ridge surface and an absorption probability of 1.3% at the side-QWs,[11] $\sim 8\times10^7$/cm-pulse carrier density is estimated per 2 μm width region within the side-QWs and the QWR at an averaged pump power of 1 kW/cm^2.

In the PL spectrum for the weakest pump power of 0.02 kW/cm^2, two spectral peaks were observed at 1.612 and 1.697 eV, which originated from the ridge QWRs and the side-QWs, respectively. As the pump power was increased, the low energy side of the PL peak from the QWRs became saturated, and the intensity of the higher energy region increased to blueshift the spectral peak. Finally at a pump power of 0.5 kW/cm^2 ($\sim 4\times10^7$ carriers/cm-pulse within the side-QWs and the QWR regions), stimulated emission was observed at 1.662 eV. This lasing energy was 50 meV higher than the ground-state PL energy of the QWRs, while it was 35 meV lower than that of the side-QWs.

In our previous paper, we studied such emission properties with micro-PL imaging technique from the cleaved edges, and assigned the origin of the stimulated emission to optical transition between excited states in the QWR.[8] In this article, we measured the top-view PL images of the ridge structure to investigate the distribution of electronic states along the wire direction.

Two contour-plot images in Fig. 2 show the top-view PL intensity mapping in the *xy* plane for a ridge laser structure at

[a]Electronic mail: watanabe@wagner.issp.u-tokyo.ac.jp
[b]Quantum Transition Project, Japan Science and Technology Corporation and Faculty of Engineering, Kagawa University, 4-6-1 Saiwaityou, Takamatsu, Kagawa 760-8526, Japan.
[c]Quantum Transition Project, Japan Science and Technology Corporation and Institute of Industrial Science, University of Tokyo, 7-22-1 Roppongi, Minato-ku, Tokyo 106-8558, Japan.

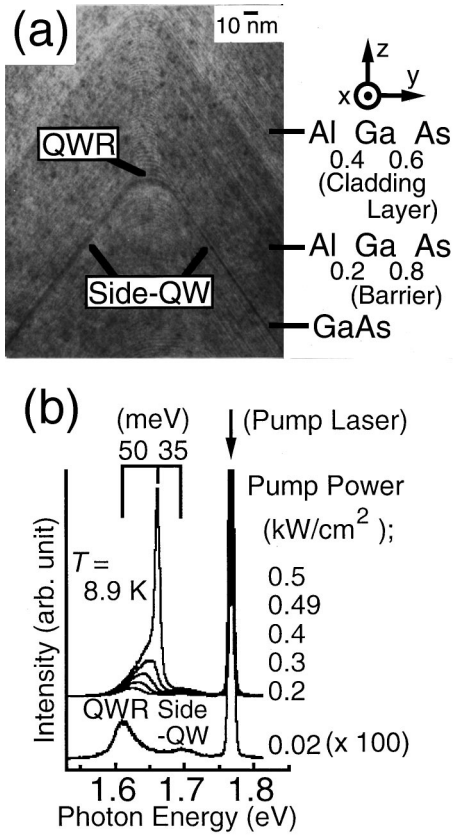

FIG. 1. (a) TEM cross-sectional image of a ridge QWR laser structure. The *x*, *y*, and *z* directions are defined as the wire direction (*x*), the lateral confinement direction (*y*), and the growth direction (*z*). (b) PL spectra at 8.9 K for the various excitation powers of 0.02, 0.2, 0.3, 0.4, 0.49, and 0.5 kW/cm^2. The sharp line due to the stimulated emission was observed at 1.662 eV for 0.5 kW/cm^2.

two PL peak energies, 1.638 eV (QWR) and 1.713 eV (side-QWs) with a bandwidth of 2 nm, at $T=4.7$ K. Uniform optical excitation by Ti:Al_2O_3 laser pulses (photon energy of 1.777 eV, excitation power of 0.07 kW/cm^2) was performed from the top of the ridge structure, and PL from the top surface was collected via an objective lens and an interference filter. The *x*, *y*, and *z* directions are the same as those defined in Fig. 1(a). The ridge wire structure is formed along the *x* direction with its cleaved edge defined as $x=0$. The images of the two adjacent side-QWs are not separated due to the spatial resolution of 1 μm of the experimental setup.[12] The PL intensity profiles along the *x* axis for the QWR and the side-QWs are shown by the green (top) and blue (bottom) lines, respectively.

The reflection image showed a uniform top-view ridge structure, which suggests that the fluctuation of vertical thickness of the ridge structure is negligible in the optical wavelength scale of $\sim\mu$m. However the PL intensity profile of the QWR showed an inhomogeneous PL pattern as can be seen in Fig. 2. Therefore the fluctuation of vertical thickness exists in the nanometer scale to perturb the quantized electronic states of the active region in the structure.

Note that the inhomogeneity of the PL pattern is in a 2–3 μm scale for the QWR, whereas that for the side-QWs is in a 1 μm scale, which is comparable to the spatial resolution of the measurement. The PL inhomogeneity results from the migration of photoexcited carriers into positions

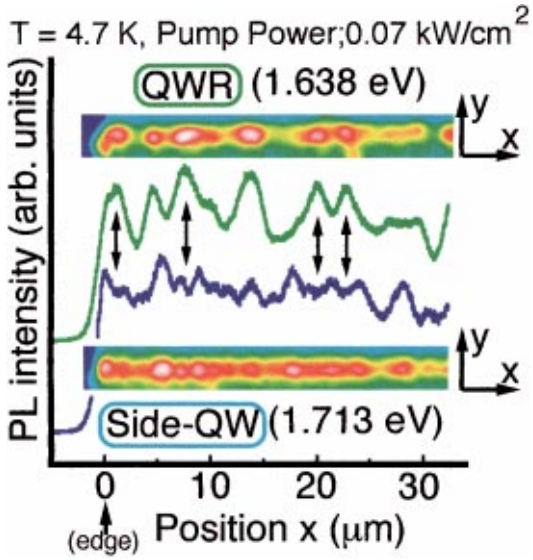

FIG. 2. Top-view PL intensity mapping in the *xy* plane for a ridge laser structure at two PL peak energies, 1.638 eV (QWR) and 1.713 eV(side-QW) with a bandwidth of 2 nm, at $T=4.7$ K. Uniform optical excitation by Ti:Al_2O_3 laser pulses (photon energy of 1.777 eV, excitation power of 0.07 kW/cm^2) was performed from the top of the ridge structure, and PL from the top surface was collected via an objective lens and an interference filter. The ridge structure is along the *x* direction with its cleaved edge defined as $x=0$. The PL intensity profiles along the *x* axis for the QWR and the side-QWs are shown by the green (top) and blue (bottom) lines, respectively.

with local energy minimum. Thus, the 2–3-μm-scale inhomogeneity indicates that the carriers are able to move along the QWR over a similar distance. We expect carrier diffusion in side-QWs along the wire direction to be inefficient, because the vertical thickness of side-QWs is thin, as is shown in Fig. 1(a).

Carrier migration from the side-QWs toward the QWR

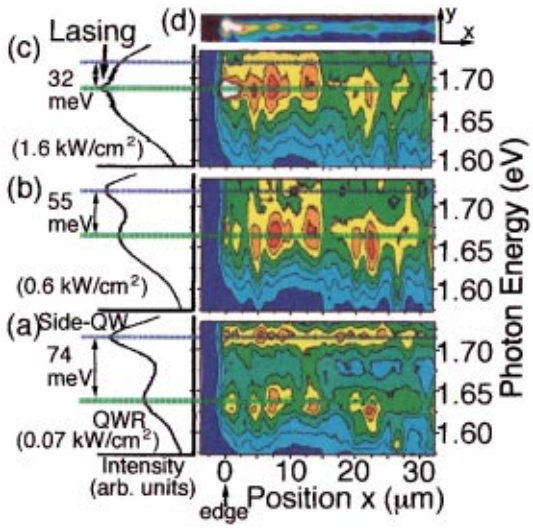

FIG. 3. The spatially and spectrally resolved PL intensity patterns at various excitation powers of (a) 0.07, (b) 0.6, and (c) 1.6 kW/cm^2, at $T=4.7$ K. The *x* axis in each image is along the wire direction, and the vertical axis represents the emission energy. The contour-plot lines in each image divide the PL intensity eight equal parts (100% as the maximum intensity of spontaneous emission in each image). The averaged PL spectrum along the *x* position is also shown on the left-hand side of each image. The contour-plot image (d) at the top shows the top-view PL image at the lasing photon energy of 1.688 eV under the same excitation power as in (c).

was also observed in the PL intensity profile. At the positions indicated by arrows in Fig. 2, the intensity of the QWR is strong while that of the side-QWs is weak. This suggests that excited carriers in the side-QWs flow efficiently into the QWR at these positions, whereas at other positions with less carrier flows, more excited carriers recombine in the side-QW regions. At the positions where PL of both QWR and side-QWs are weak, it is interpreted that carriers flowed away along the wire direction or recombined via nonradiative decay processes.

Three contour-plot images (a)–(c) in Fig. 3 represent the spatially and spectrally resolved PL intensity patterns at various excitation powers of (a) 0.07–(c) 1.6 kW/cm^2, at $T=4.7$ K. The x axis in each image is along the wire direction, and the vertical axis represents the emission energy. To construct each image, we measured the PL intensity profiles along the x axis as in Fig. 2 at every 5 meV of photon energies, and arranged them in rows.

The averaged PL spectrum along the all x position is also shown on the left-hand side of each image. The contour-plot image [Fig. 3(d)] at the top shows the top-view PL image like those in Fig. 2 at the lasing photon energy of 1.688 eV under the same excitation power as in Fig. 3(c).

At the weak excitation power of 0.07 kW/cm^2 [Fig. 3(a)], two peaks inherent in QWRs and side-QWs are shown in the averaged spectrum. As for the QWR, each inhomogeneous PL center has different spectral peak energy due to a small difference of QWR volume at each wire position, which explains why the averaged spectrum is broad. The PL intensity profiles along the wire at the photon energy of the QWR and the side-QWs show the spatial inhomogeneity of electronic states of the QWR and the side-QWs.

At stronger excitation power of 0.6 kW/cm^2 [Fig. 3(b)], the averaged spectrum shows that the spectral energy peak of the QWR blueshifts while that of the side-QWs does not move. The PL intensity profile at the blueshifted energy peak of the QWR marked by the green (bottom) line in Fig. 3(b) is very similar to that of the QWR ground state emission marked by the green (bottom) line in Fig. 3(a), which suggests that the blueshifted PL is due to the transition between the excited states of QWRs.

Then, at the strongest excitation power of 1.6 kW/cm^2 [Fig. 3(c)], lasing was observed in the averaged spectrum at a further blueshifted energy of 1.688 eV, which is similar to the result of Fig. 1(b). The intensity of the sharp lasing spectrum is small in Fig. 3(c), since the detection was achieved in the top-view configuration.

Note the top-view spontaneous emission profile at the lasing energy marked by the green line (bottom) in Fig. 3(c). It is almost the same as those of the ground and excited states of QWR emission profiles observed at the green (bottom) lines in Figs. 3(a) and 3(b). Therefore, the origin of stimulated emission can be safely assigned as the excited states of the QWR, instead of the low-energy tail of the side-QW optical transition. This result strongly supports our former result.[8]

In the spatial image [Fig. 3(d)] and the spatially and spectrally resolved PL intensity patterns [Fig. 3(c)], strong stimulated emission signal was observed at the cleaved edge position ($x=0$ μm). Although the lasing occurs in the ridge waveguide direction, the output light emitted from the cleaved edge diverges. Therefore, the large numerical aperture collection optics makes it possible to observe stimulated emission even in the top-view configuration. Note that there is no scattered stimulated emission on the ridge waveguide structure ($x>0$ μm). This means that there are no significant scatterers in the ridge waveguide structure which cause scattering of light in the cavity and hence cause optical losses.

The results shown in Fig. 3 again demonstrate that the fluctuation of vertical thickness of the ridge structures is negligible in the optical wavelength scale of $\sim\mu$m, while it exists in the scale of $\sim$nm to perturb the electronic states of the active regions in the structures.

In summary, the electronic states distribution of QWRs along the wire direction was investigated using the top-view PL imaging method. The fluctuation of vertical thickness was in the scale of $\sim$nm, resulting in the inhomogeneous electronic states in spite of the uniform optical waveguide. The inhomogeneous PL caused by carrier diffusion over a few μm in QWR structures was observed, proving that the QWR is connected over this distance. Spatially and spectrally resolved PL intensity patterns above and below the lasing threshold supports that the origin of stimulated emission is the transition between the excited states of QWRs.

The authors would like to thank Professor P. M. Petroff (UCSB) for valuable discussions and suggestions, and would also like to thank Dr. T. Ozaki (ISSP) for critically reading the manuscript. This work is partly supported by a Grant-in-Aid from the Ministry of Education, Science, Sports, and Culture, Japan. One of the authors (S.W.) would like to thank JSPS for the partial financial support.

[1] E. Kapon, D. M. Hwang, and R. Bhat, Phys. Rev. Lett. **63**, 430 (1989).
[2] W. Wegscheider, L. N. Pfeiffer, M. M. Dignam, A. Pinczuk, K. W. West, S. L. McCall, and R. Hull, Phys. Rev. Lett. **71**, 4071 (1993).
[3] A. Chavez-Pirson, H. Ando, H. Saito, and H. Kanbe, Appl. Phys. Lett. **64**, 1759 (1994).
[4] W. Wegscheider, L. Pfeiffer, K. West, and R. E. Leibenguth, Appl. Phys. Lett. **65**, 2510 (1994).
[5] S. Hara, J. Motohisa, and T. Fukui, Electron. Lett. **34**, 894 (1998).
[6] E. Kapon, in *Semiconductor Lasers I: Fundamentals*, edited by E. Kapon (Academic, Boston, 1999), Chap. 4, pp. 291–360.
[7] S. Koshiba, S. Watanabe, Y. Nakamura, M. Yamauchi, M. Yoshita, M. Baba, H. Akiyama, and H. Sakaki, J. Cryst. Growth **201/202**, 810 (1999).
[8] S. Watanabe, S. Koshiba, M. Yoshita, H. Sakaki, M. Baba, and H. Akiyama, Appl. Phys. Lett. **73**, 511 (1998).
[9] R. D. Grober, T. D. Harris, J. K. Trautman, E. Betzig, W. Wegscheider, L. Pfeiffer, and K. West, Appl. Phys. Lett. **64**, 1421 (1994).
[10] U. Ben-Ami, R. Nagar, N. Ben-Ami, J. Scheuer, M. Orenstein, G. Eisenstein, A. Lewis, E. Kapon, F. Reinhardt, P. Ils, and A. Gustafsson, Appl. Phys. Lett. **73**, 1619 (1998).
[11] Y. Masumoto, M. Matsuura, S. Tarucha, and H. Okamoto, Phys. Rev. B **32**, 4275 (1985).
[12] M. Yoshita, H. Akiyama, T. Someya, and H. Sakaki, J. Appl. Phys. **83**, 3777 (1998).